

See discussions, stats, and author profiles for this publication at: <https://www.researchgate.net/publication/51491814>

Simultaneous Interactions of Anions and Cations with Cyclohexane and Adamantane: Aliphatic Cyclic Hydrocarbons as Charge Insulators

ARTICLE in THE JOURNAL OF PHYSICAL CHEMISTRY A · JULY 2011

Impact Factor: 2.69 · DOI: 10.1021/jp205300c · Source: PubMed

CITATIONS

8

READS

31

4 AUTHORS:



[Cristina Trujillo](#)

Trinity College Dublin

36 PUBLICATIONS 392 CITATIONS

[SEE PROFILE](#)



[Goar Sánchez](#)

University College Dublin

69 PUBLICATIONS 900 CITATIONS

[SEE PROFILE](#)



[Ibon Alkorta](#)

Spanish National Research Council

679 PUBLICATIONS 12,389 CITATIONS

[SEE PROFILE](#)



[José Elguero](#)

Spanish National Research Council

1,502 PUBLICATIONS 22,151 CITATIONS

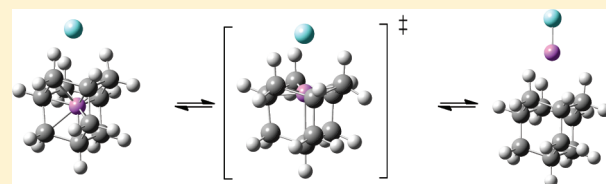
[SEE PROFILE](#)

Simultaneous Interactions of Anions and Cations with Cyclohexane and Adamantane: Aliphatic Cyclic Hydrocarbons as Charge Insulators

Cristina Trujillo, Goar Sánchez-Sanz, Ibon Alkorta,* and José Elguero

Instituto de Química Médica (CSIC), Juan de la Cierva, 3, E-28006 Madrid, Spain

ABSTRACT: With ab initio MP2 computational methods, a theoretical study has been carried out to characterize the interaction between aliphatic cyclic hydrocarbons, as models of molecular hydrocarbon monolayers, with cations (Li^+ , Na^+ , and K^+), anions (F^- , Cl^- , and Br^-), and both simultaneously in opposite faces of the hydrocarbons. In addition, the energetic barrier for the cation crossing through the hydrocarbon ring has been calculated. The hydrocarbons chosen for this study are cyclohexane (C_6H_{12}) and adamantane ($\text{C}_{10}\text{H}_{16}$). The energies obtained for the $\text{M}^+:\text{hydrocarbon}:X^-$ complexes indicate positive cooperativity in the cases where the hydrocarbon is cyclohexane while diminutive effects are found in the adamantane complexes. The density functional theory–symmetry adapted perturbation theory analysis of the interaction energies shows that the most important term in the complexes with cations is the induction, while in the complexes with anion and with cations and anions simultaneously the most important term is the repulsion-exchange one. The electron density of the complexes has been analyzed using the atoms in molecules methodology and provides some insight to the electron transfer within the complexes.



INTRODUCTION

The possibility of using molecular monolayers has been widely developed in recent years with the discovery and potential applications of graphene.¹ There is a logical path connecting graphite → graphene → benzene, another path connecting diamond → diamondoids² → adamantane, and finally a path connecting diamond → hydrogenated graphene (graphane)^{3–5} → cyclohexane (Figure 1). It is well-known that diamond is an excellent insulator⁶ and graphene in vacuum is also an insulator.^{7,8} Moreover, to improve lithium batteries, it is necessary to increase our knowledge on the permeability of monolayers of carbon derivatives to cations such as Li^+ .⁹

The importance of the interaction of cations with aromatic systems has been recognized for a long time.^{10–12} More recently, the possibility of interaction of anions with aromatic systems has been explored theoretically and described experimentally.^{13–16} A combination of these two types of interactions has been studied by locating anions and cations in different faces of the aromatic ring.^{17–23} In these cases, the aromatic molecule acts as insulator of the ions and can be used as a way to store “information” between the charged systems.

In those cases where the molecule that acts as an insulator has a cage shape, the sequestration of ions can be achieved. The inclusion of cations and anions in the C_{60} fullerene has been described in the literature.^{24–27} Recently, the $\text{Li}^+:\text{C}_{60}:\text{SbCl}_6^-$ complex has been described where the lithium cation is located inside the fullerene while the SbCl_6^- anion lies outside.²⁸ Moran et al.²⁹ theoretically study hydrocarbon cage complexes and found that adamantane was the smallest cage capable of encapsulating a wide variety of endohedral atoms and ions, including He and Li^+ . Further studies have been carried out on the

characteristics of atoms enclosed in the adamantane cage by Bader and Fang³⁰ including the Li^+ :adamantane complex, and the mechanism of the reaction path from the inclusion complex $\text{He}:\text{adamantane}$ to its two separated components have been recently reported.³¹

In the present article, the potential use of two simple hydrocarbons, adamantane ($\text{C}_{10}\text{H}_{16}$) and cyclohexane, C_6H_{12} (see Figure 1), as a model of a more extended system such as diamondoids and graphane, as potential charge isolators has been explored. Thus, the complexes formed with Li^+ in one side of the hydrocarbon and anions (F^- , Cl^- , and Br^-) in the other side have been studied. In addition, the barrier to transfer the lithium cation from one side to the other of the hydrocarbon system has been calculated. Therefore, we consider cyclohexane and adamantane as models of the monolayers and because of this we leave aside ways going around the molecules.

2. COMPUTATIONAL DETAILS

The geometry of monomers and complexes has been fully optimized with the Gaussian09 program using the standard 6-311++G(d,p) basis sets³² at the second-order Moller–Plesset level.³³ Harmonic vibrational frequencies were computed at the same level used for the geometry optimizations to classify the stationary points either as local minima or transition states (TS).

Special Issue: Richard F. W. Bader Festschrift

Received: June 6, 2011

Revised: June 28, 2011

Published: July 14, 2011

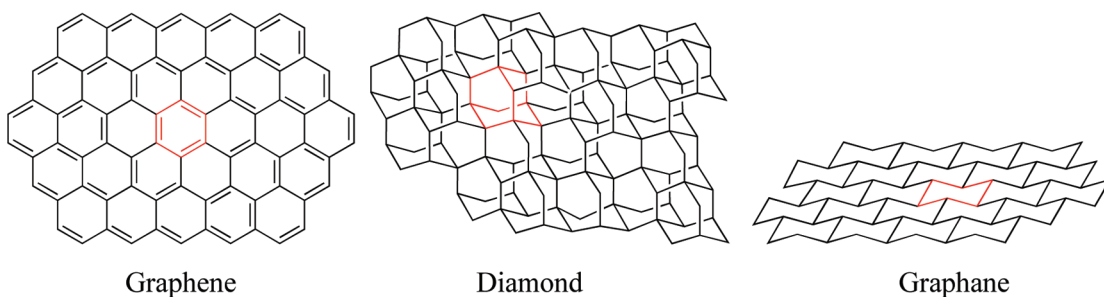


Figure 1. Sheets formed by benzenes (graphene), adamantanes (diamond), and cyclohexanes (graphane).

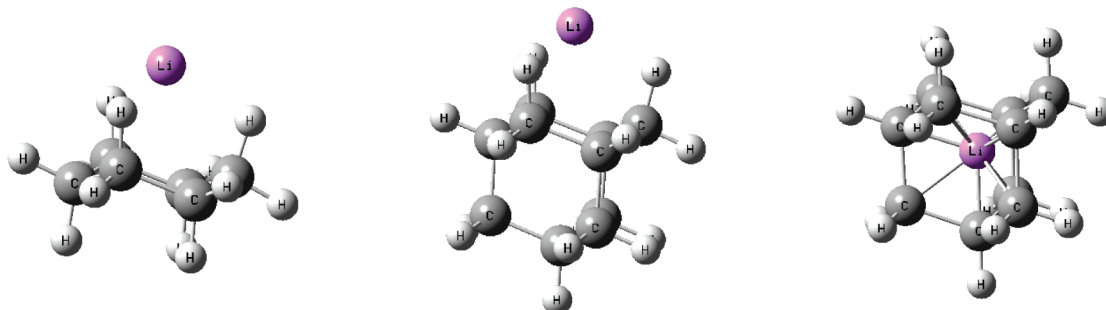


Figure 2. Complexes of lithium cation with cyclohexane and adamantane optimized at the MP2/6-311++G(d,p) computational level.

Table 1. Interaction Energy (kJ mol^{-1}) of the Hydrocarbon: M^+ Complexes Calculated at the MP2/6-311++G(3df,2p) Computational Level^a

system	E_i (kJ mol^{-1})	$E_i +$ BSSE	distance $\text{M}^+ \dots \text{H}$	distance $\text{M}^+ \dots \text{C}$
$\text{C}_6\text{H}_{12}:\text{Li}^+$	-83.6	-79.9	1.880	2.371
$\text{C}_6\text{H}_{12}:\text{Na}^+$	-41.9	-38.6	2.325	3.147
$\text{C}_6\text{H}_{12}:\text{K}^+$	-29.2	-27.2	2.718	3.632
$\text{C}_{10}\text{H}_{16}:\text{Li}^+$ (in)	286.3	303.6		1.645
$\text{C}_{10}\text{H}_{16}:\text{Li}^+$ (out)	-92.0	-88.6	1.846	2.336
$\text{C}_{10}\text{H}_{16}:\text{Na}^+$ (in)	1372.0	1393.6		1.801
$\text{C}_{10}\text{H}_{16}:\text{Na}^+$ (out)	-46.8	-43.4	2.308	3.165
$\text{C}_{10}\text{H}_{16}:\text{K}^+$ (out)	-33.6	-31.2	2.693	3.631

^aThe distances of the cations to the closest hydrogen and carbon atoms are included (\AA).

In order to have a good description of the energies, a single point calculation at the MP2/6-311++G(3df,2p) computational level has been carried out for the monomers and complexes. Using these values, the interaction energies have been calculated as the difference between the total energy of the complex and the sum of the isolated monomers. They have been corrected for the inherent basis set superposition error (BSSE) using the Boys-Bernardi counterpoise technique.³⁴

Density functional theory—symmetry adapted perturbation theory (DFT-SAPT) calculations³⁵ have been carried out, in order to obtain detailed information of the different contributions to the total interaction energy. The SAPT methodology separates the interaction energy into several components, which are related to physical variables such as dispersion, electrostatic, induction, and exchange. The SAPT interaction energy can be

Table 2. DFT-SAPT Energy Components (kJ mol^{-1}) of the Interaction of the Hydrocarbons with Cations

X	$E_{\text{el}}^{(1)}$	$E_{\text{ex}}^{(1)}$	$E_i^{(2)}$	$E_D^{(2)}$	$\delta(\text{HF})$
$\text{C}_6\text{H}_{12}:\text{Li}^+$	-22.65	56.77	-121.46	-3.31	-6.65
$\text{C}_6\text{H}_{12}:\text{Na}^+$	-7.20	23.39	-61.15	-1.44	1.52
$\text{C}_6\text{H}_{12}:\text{K}^+$	-3.74	21.03	-36.82	-3.06	0.67
$\text{C}_{10}\text{H}_{16}:\text{Li}^+$ (in)	22.75	606.76	-340.04	-28.18	-72.44
$\text{C}_{10}\text{H}_{16}:\text{Li}^+$ (out)	-25.30	63.04	-135.29	-3.75	-8.02
$\text{C}_{10}\text{H}_{16}:\text{Na}^+$ (in)	-376.25	1421.62	-279.81	-16.45	49.27
$\text{C}_{10}\text{H}_{16}:\text{Na}^+$ (out)	-5.62	23.41	-67.00	-1.53	1.24
$\text{C}_{10}\text{H}_{16}:\text{K}^+$ (out)	-3.33	22.02	-41.56	-8.32	0.63

written as the sum of the truncated expansion terms

$$E_{\text{int}} = E_{\text{pol}}^{(1)} + E_{\text{ex}}^{(1)} + E_{\text{ind}}^{(2)} + E_{\text{ex-ind}}^{(2)} + E_{\text{disp}}^{(2)} \\ + E_{\text{ex-disp}}^{(2)} + \delta(\text{HF})$$

Those terms can be associated to some physical quantities using the relationships

$$E_{\text{elec}} = E_{\text{pol}}^{(1)}$$

$$E_{\text{ind}} = E_{\text{ind}}^{(2)} + E_{\text{ex-ind}}^{(2)}$$

$$E_{\text{disp}} = E_{\text{disp}}^{(2)} + E_{\text{ex-disp}}^{(2)}$$

$$E_{\text{ex}} = E_{\text{ex}}^{(1)}$$

where $E_{\text{pol}}^{(1)}$ is the electrostatic energy of monomers with the unperturbed electron distribution, $E_{\text{ex}}^{(1)}$ is the first-order valence repulsion energy of the monomers due to the Pauli

exclusion principle, $E_{\text{ind}}^{(2)}$ denotes the second-order energy resulting from the induction interaction, and $E_{\text{ex-ind}}^{(2)}$ accounts for the repulsion change caused by the electronic cloud deformation, $E_{\text{disp}}^{(2)}$ stands for the second-order dispersion energy, and finally, $E_{\text{ex-disp}}^{(2)}$ represents the second-order correction for a coupling between the exchange repulsion and the dispersion interactions. The $\delta(\text{HF})$ term is a Hartree–Fock correction, which includes higher order induction and exchange corrections. These computations have been carried out using the PBE0/aug-cc-pVDZ computational level within the MOLPRO program.³⁶

The bonding characteristics have been analyzed by means of the atoms in molecules (AIM) theory.^{37,38} For this purpose we have located the most relevant bond critical points (BCP) and evaluated the electron density at each of them by means of the AIMPAc and MORPHY programs.^{39–41} The natural bond orbital (NBO) method⁴² has been used to derived the atomic charges and to analyze the orbital interactions using the NBO 3.1 program⁴³ implemented in the Gaussian-09 package.

■ RESULTS AND DISCUSSION

Hydrocarbon: M^+ Complexes. First, we have studied the interaction between the two hydrocarbons, cyclohexane (C_6H_{12}) and adamantane ($C_{10}H_{16}$) and the metal cations, the Li^+ , Na^+ , and K^+ . Two configurations for the adamantane complexes, with

Table 3. Electron density properties (a.u.) of the intermolecular BCPs, charge of the metallic atom (e) calculated with the AIM and NBO methods and extend of the electron overlap (Å) of the hydrocarbon: M^+ complexes calculated at MP2/6-311++G(d,p) computational level

system	$M^+ \cdots H/C$ (BCP)		charge of M^+		
	ρ	$\nabla^2 \rho$	AIM	NBO	overlap
$C_6H_{12}:\text{Li}^+$	0.0157	0.0935	0.938	0.879	1.14
$C_6H_{12}:\text{Na}^+$	0.0081	0.0403	0.955	0.956	0.54
$C_6H_{12}:\text{K}^+$	0.0037	0.0134	0.965	0.980	0.43
$C_{10}H_{16}:\text{Li}^+$ (out)	0.0171	0.1034	0.934	0.880	1.21
$C_{10}H_{16}:\text{Na}^+$ (out)	0.0083	0.0413	0.953	0.958	0.54
$C_{10}H_{16}:\text{K}^+$ (out)	0.0075	0.0279	0.963	0.982	0.45
$C_{10}H_{16}:\text{Li}^+$ (in)	0.0659 ^a	0.4725	0.814	0.176	
$C_{10}H_{16}:\text{Na}^+$ (in)	0.0557 ^a	0.3680	0.751	0.226	

^aThese values correspond to $M^+ \cdots C$ interactions.

the cations outside and inside the molecular cage, have been considered (Figure 2). The complexes obtained present C_{3v} symmetry, except those with the cation inside the adamantane which shows T_d symmetry.

The interaction energies of these complexes have been gathered in Table 1. Negative interaction energies have been obtained for the cyclohexane complexes and for the complexes with the cation in the outer side of adamantane. In contrast, positive interaction energies have been found for those complexes with the cations inside the adamantane molecule. While those of lithium and sodium inside adamantane complexes are local minima, the potassium one is not. The interaction energies obtained for the minima configurations range between -89 and $+1394 \text{ kJ mol}^{-1}$.

The most negative (or less positive) interaction energies for the complexes with a given hydrocarbon and interaction type are obtained for the Li^+ followed by the Na^+ , the less favorable complexes being those of the K^+ . The complexes formed with the cyclohexane and those in the outer part of the adamantane show similar interaction energies for a given cation, with the latter ones being slightly more stable.

The different size of the cations is clearly reflected by the intermolecular distances found in the complexes. Thus, shorter distances are found in the Li^+ complexes than in the Na^+ ones, those of K^+ being the largest ones. Comparison of the distances in the cyclohexane complexes and those in the outer face adamantane complexes shows that for the same cation, shorter $M^+ \cdots H$ distances are found in the latter than in the former, in agreement with the interaction energies found.

The complexation of the cations with the cyclic hydrocarbons produces an important elongation of the interacting C–H bond (up to 0.1 Å in the Na^+ complexes). The NBO analysis of these complexes indicates that this effect is due to a charge transfer from the C–H bond to the empty orbitals of the cation which weakens the bond producing its elongation. In those cases where the cations are inside the adamantane, the C–C bonds are elongated 0.07 Å when the metallic cation is Li^+ and 0.21 Å when it is Na^+ .

The DFT-SAPT analysis (Table 2) shows for the cyclohexane complexes and for the outer face of adamantane that the dominant attractive energy term is the induction, $E_i^{(2)}$, which represents 78–90% of the total attraction forces. The electrostatic energy, $E_{el}^{(1)}$, is the second most important contribution ranging between a 6 and 15% of the total attractive terms. The smaller attractive contribution corresponds to the dispersion, $E_D^{(2)}$, except for the $C_{10}H_{16}:\text{K}^+$ (out) complex where it is larger

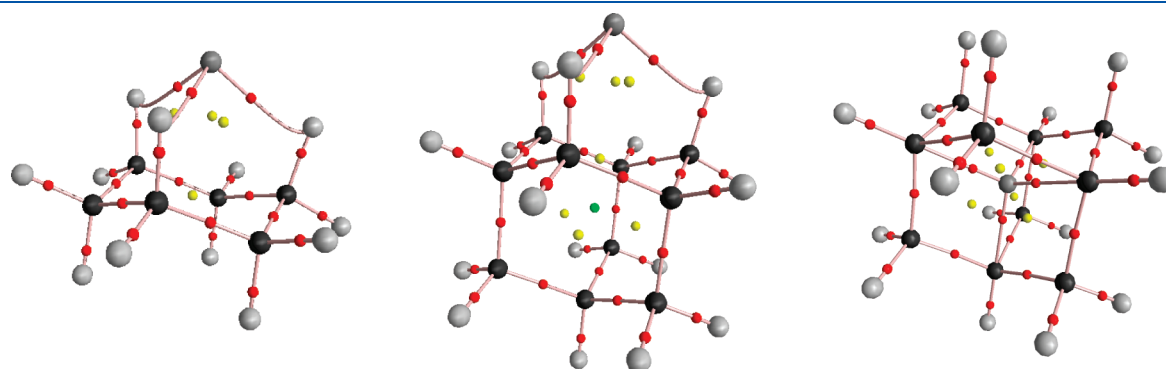


Figure 3. Molecular graph of the Li^+ complexes calculated at the MP2/6-311++G(d,p) computational level.

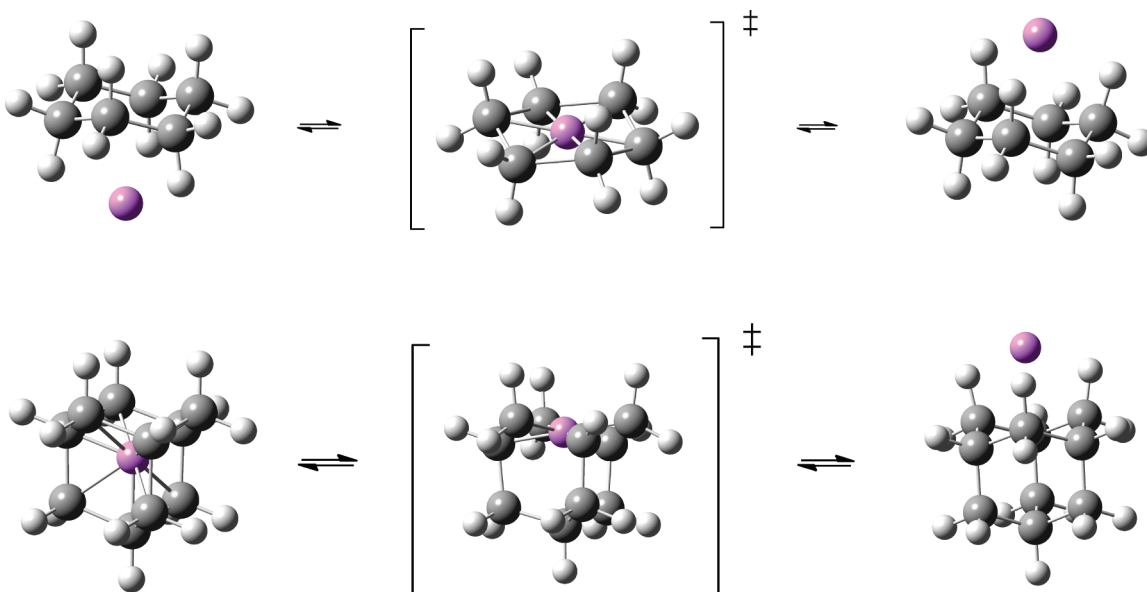


Figure 4. Optimized geometries at the MP2/6-311++G(d,p) computational level of the stationary structures of the cation crossing process.

Table 4. Interaction Energy (kJ mol^{-1}) of the Hydrocarbon: X^- Complexes Calculated at the MP2/6-311++G(3df,2p) Computational Level and Intermolecular Distances (\AA) between the Anion and the Closest Hydrocarbons Atoms

system	E_i (kJ mol^{-1})	$E_i +$ BSSE	distance $\text{X}^- \cdots \text{H}$	distance $\text{X}^- \cdots \text{C}$
$\text{C}_6\text{H}_{12}:\text{F}^-$	-64.9	-54.1	2.187	3.127
$\text{C}_6\text{H}_{12}:\text{Cl}^-$	-36.7	-32.0	2.736	3.706
$\text{C}_6\text{H}_{12}:\text{Br}^-$	-30.3	-27.4	2.944	3.925
$\text{C}_{10}\text{H}_{16}:\text{F}^-$ (in)	1587.0	1636.9		1.713
$\text{C}_{10}\text{H}_{16}:\text{F}^-$ (out)	-72.7	-60.2	2.153	3.101
$\text{C}_{10}\text{H}_{16}:\text{Cl}^-$ (out)	-42.4	-35.3	2.696	3.673
$\text{C}_{10}\text{H}_{16}:\text{Br}^-$ (out)	-35.2	-30.8	2.899	3.889

than $E_{\text{el}}^{(1)}$. In the case of the complexes with the cation inside the adamantane cage, the exchange term, $E_{\text{ex}}^{(1)}$, became so large that the attractive contribution cannot compensate its value. The results obtained here are similar to those reported for the cation- π complexes where the dominant attractive term is the dispersion followed by far by the electrostatic one,^{44–46} and also for the model system $\text{Li}^+:\text{CH}_4$, computed in the present article, where the $E_i^{(2)}$ term has a value of -54 kJ/mol while the $E_{\text{el}}^{(1)}$ is only -20 kJ/mol calculated with the aug-cc-pVQZ basis set (almost identical results are obtained for the aug-cc-pVDZ and aug-cc-pVTZ basis sets).

The topological analysis of the electron density shows the presence of intermolecular bond critical points (BCPs) between the metal cations and the closest hydrogen atoms in the complexes with cyclohexane and outer face adamantane (Table 3 and Figure 3). In contrast, the complexes with the cations inside the adamantane show BCPs between the cations and four of the carbon atoms.

Using the electron density surface at 0.001 au for the isolated cations and along the C_{3v} symmetry axes of the hydrocarbons, the extent of the electron density overlap within the complexes can be estimated. The largest overlap is observed in

Table 5. DFT-SAPT Energy Components (kJ mol^{-1}) of the Interaction of the Hydrocarbons with Anions

X	$E_{\text{el}}^{(1)}$	$E_{\text{ex}}^{(1)}$	$E_i^{(2)}$	$E_D^{(2)}$	$\delta(\text{HF})$
$\text{C}_6\text{H}_{12}:\text{F}^-$	-61.36	97.91	-55.10	-26.66	-7.26
$\text{C}_6\text{H}_{12}:\text{Cl}^-$	-35.12	61.35	-27.36	-24.67	-5.72
$\text{C}_6\text{H}_{12}:\text{Br}^-$	-29.02	50.94	-21.43	-23.01	-5.16
$\text{C}_{10}\text{H}_{16}:\text{F}^-$ (out)	-65.46	105.82	-62.57	-28.34	-8.23
$\text{C}_{10}\text{H}_{16}:\text{Cl}^-$ (out)	-37.61	66.76	-31.97	-26.47	-6.48
$\text{C}_{10}\text{H}_{16}:\text{Br}^-$ (out)	-31.23	55.77	-25.40	-24.86	-5.84

Table 6. Electron Density Properties at the BCP (a.u.), Charge of the Anion (e), and Electron Density Overlap (\AA) of the Hydrocarbon: X^- Complexes Calculated at the MP2/6-311++G(d,p) Level

system	H \cdots X interaction		charge of X^-		
	ρ_{BCP}	$\nabla^2\rho_{\text{BCP}}$	AIM	NBO	overlap
$\text{C}_6\text{H}_{12}:\text{F}^-$	0.017	0.053	-0.950	-0.957	1.13
$\text{C}_6\text{H}_{12}:\text{Cl}^-$	0.010	0.028	-0.935	-0.970	0.92
$\text{C}_6\text{H}_{12}:\text{Br}^-$	0.005	0.015	-0.937	-0.973	0.78
$\text{C}_{10}\text{H}_{16}:\text{F}^-$ (in)	0.180 ^a	-0.029 ^a	-0.657	-0.665	
$\text{C}_{10}\text{H}_{16}:\text{F}^-$ (out)	0.018	0.057	-0.947	-0.952	1.18
$\text{C}_{10}\text{H}_{16}:\text{Cl}^-$ (out)	0.011	0.031	-0.930	-0.966	0.98
$\text{C}_{10}\text{H}_{16}:\text{Br}^-$ (out)	0.009	0.023	-0.932	-0.970	0.84

^a These values correspond to F \cdots C interactions.

the Li^+ complexes with values of 1.14 and 1.21 \AA for the cyclohexane and adamantane complexes. The overlap in the Na^+ and K^+ complexes ranges between 0.54 and 0.43 \AA being slightly larger in the Na^+ than in the K^+ systems.

The amount of charge transferred from the hydrocarbons to the cations is gathered in Table 3. Similar charges are obtained for

Table 7. Interaction Energy, Cooperativity Effect (kJ mol^{-1}), and Intermolecular Distances (\AA) Calculated at the MP2/6-311++G(3df,2p) Level

system	E_1	$E_{\text{I+BSSE}}$	$\text{X}^-:\text{Li}^+$ energy ^a	E_{coop}	intermolecular distances		
					$\text{X}^- \cdots \text{H}$	$\text{M}^+ \cdots \text{H/C}$	$\text{X}^- \cdots \text{M}^+$
$\text{F}^-:\text{C}_6\text{H}_{12}:\text{Li}^+$	-510.8	-491.0	-333.2	-23.8	1.906	1.833	4.285
$\text{Cl}^-:\text{C}_6\text{H}_{12}:\text{Li}^+$	-439.5	-425.9	-293.7	-20.3	2.417	1.851	4.910
$\text{Br}^-:\text{C}_6\text{H}_{12}:\text{Li}^+$	-421.2	-410.4	-283.3	-19.8	2.581	1.851	5.118
$\text{F}^-:\text{C}_{10}\text{H}_{16}:\text{Li}^+$	-154.4	-121.0	-421.9	57.5	1.898	1.637 ^b	3.440
$\text{Cl}^-:\text{C}_{10}\text{H}_{16}:\text{Li}^+$	-81.3	-53.2	-366.7	45.2	2.388	1.638 ^b	4.024
$\text{Br}^-:\text{C}_{10}\text{H}_{16}:\text{Li}^+$	-62.0	-37.5	-352.0	41.7	2.559	1.639 ^b	4.232

^a Interaction energy of the $\text{X}^-:\text{Li}^+$ system at the same disposition found in the complexes. ^b $\text{M}^+ \cdots \text{C}$ distance.

Table 8. DFT-SAPT Energy Components (kJ mol^{-1}) of the Simultaneous Interaction of the Cations and Anions with the Hydrocarbons

X	$E_{\text{el}}^{(1)}$	$E_{\text{ex}}^{(1)}$	$E_i^{(2)}$	$E_D^{(2)}$	$\delta(\text{HF})$
$\text{F}^-:\text{C}_6\text{H}_{12}:\text{Li}^+$	-260.94	454.64	-270.86	-72.03	-32.34
$\text{Cl}^-:\text{C}_6\text{H}_{12}:\text{Li}^+$	-227.14	397.58	-242.13	-74.32	-29.06
$\text{Br}^-:\text{C}_6\text{H}_{12}:\text{Li}^+$	-234.61	404.92	-245.54	-77.27	-30.40
$\text{F}^-:\text{C}_{10}\text{H}_{16}:\text{Li}^+$	-254.12	1008.04	-485.84	-99.49	-84.88
$\text{Cl}^-:\text{C}_{10}\text{H}_{16}:\text{Li}^+$	-236.47	979.92	-520.88	-106.66	-71.38
$\text{Br}^-:\text{C}_{10}\text{H}_{16}:\text{Li}^+$	-259.86	1003.09	-572.24	-111.75	-62.18

the cations when they are located outside of adamantane or interacting with cyclohexane, ranging the charge transferred between 0.062 and 0.035 e, with the smaller values being those of the larger metallic atoms. In contrast, very large charge transfers are observed in those cases when the cations are inside the adamantane cage due to the proximity of the donor CH_2 groups of the hydrocarbon to the cations.

In contrast, the charge transferred in the complexes with the metallic cations inside the adamantane is much larger, being 0.25 e in the Na^+ complex and 0.19 e in the Li^+ one.

The possibility of the cations crossing the hydrocarbon ring has been explored (Figure 4). Other possible mechanisms have not been considered since the studied systems represent models of extended monolayers such as those found in graphane. Only in the case of Li^+ have true TS structures been found, while for the rest of the cations this process is associated to the destruction of the hydrocarbon and the structures obtained present several imaginary frequencies. Thus, in the rest of the article, only the Li^+ will be considered. The barrier obtained for the Li^+ transfer has been 485, 143, and 521 kJ mol^{-1} for the crossing starting from the cyclohexane complex, the inside adamantane, and the outer adamantane complexes, respectively. The large values of the barriers indicate that these hydrocarbons can effectively be used to store a certain density of cations in each side of them.

Hydrocarbon: X^- Complexes. As in the case of the cations, the possibility to find stable structures in the interactions between the anions (F^- , Cl^- , and Br^-) and the hydrocarbons has been explored. Minimum energy structures with C_{3v} symmetry have been obtained for the complexes with cyclohexane and the outer face of adamantane. Inside the adamantane cage, only the F^- has been found to be an energetic minimum

structure, while the complexes with the rest of the anions (Cl^- and Br^-) present several imaginary frequencies.

The relative energies of the complexes formed with respect to the isolated anion and hydrocarbons are gathered in Table 4. The range of the interaction energies in the attractive complexes is similar to those found for the metallic cations, with the hydrocarbon: X^- being slightly smaller than the corresponding hydrocarbon: M^+ when X and M are in the same row of the periodic table. The only minimum found with the anion inside the adamantane molecule corresponds to the complex with F^- , and it is very unstable compared to the isolated adamantane and F^- atoms. Thus, it will not be considered for the rest of the article.

As in the case of the complexes with cations, the intermolecular distances are clearly dominated by the size of the anions and slightly shorter distances are found in the complexes with adamantane than with cyclohexane. The complex formation does not produce significant changes in the geometry of the hydrocarbons in contrast with the effect observed in the complexes with the metallic cations.

The DFT-SAPT analysis of these complexes (Table 5) shows that the largest component of the interaction energy, in absolute value, corresponds to the exchange, $E_{\text{ex}}^{(1)}$. Among, the attractive terms, the electrostatic one, $E_{\text{el}}^{(1)}$, is slightly more important than the induction component, $E_i^{(2)}$. The DFT-SAPT results found for the $\text{F}^-:\text{CH}_4$ model system with the aug-cc-pVQZ basis set are in line with those reported in Table 5, showing a larger value for $E_{\text{el}}^{(1)}$ than for $E_i^{(2)}$. The results reported in the literature for the SAPT analysis in anion: π complexes⁴⁷ have shown that the $E_{\text{el}}^{(1)}$ is the most important attractive term when the anion is fluoride while in the cases of chloride and bromide the $E_i^{(2)}$ is slightly more important.

A comparison of the values obtained in the complexes with the anions with those of the cations shows that the importance of the electrostatic and induction terms is reversed and that the dispersion terms are much larger in absolute value in the former cases than in the latter.

The topological analysis of the electron density shows a similar pattern to that found in the case of the cation complexes with the presence of three anion: $\cdots \text{H}$ interactions for the cyclohexane and outer face of adamantane. In the case of the inner face adamantane complex with F^- , the anion is simultaneously connected with the closest four carbon atoms.

Interactions with the hydrogen atoms (Table 6) are similar to those described for hydrogen bond interactions,⁴⁸ with values of the electron density between 0.005 and 0.018 and positive values

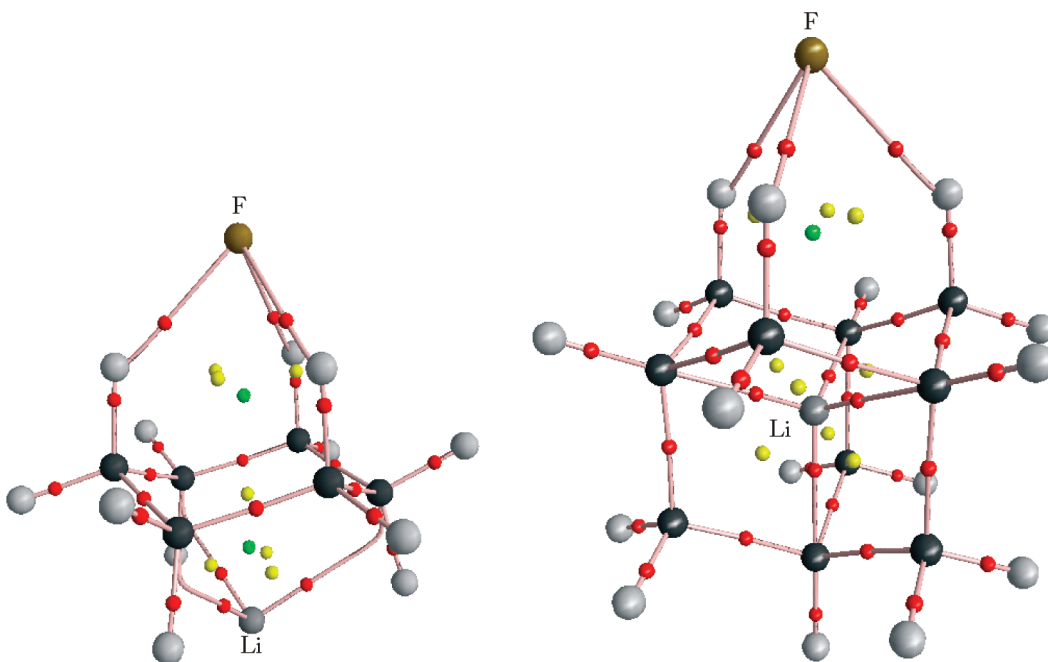


Figure 5. Molecular graph of the $\text{F}^-:\text{C}_6\text{H}_{12}:\text{Li}^+$ and $\text{F}^-:\text{C}_{10}\text{H}_{16}:\text{Li}^+$ complexes calculated at the MP2/6-311++G(d,p) computational level.

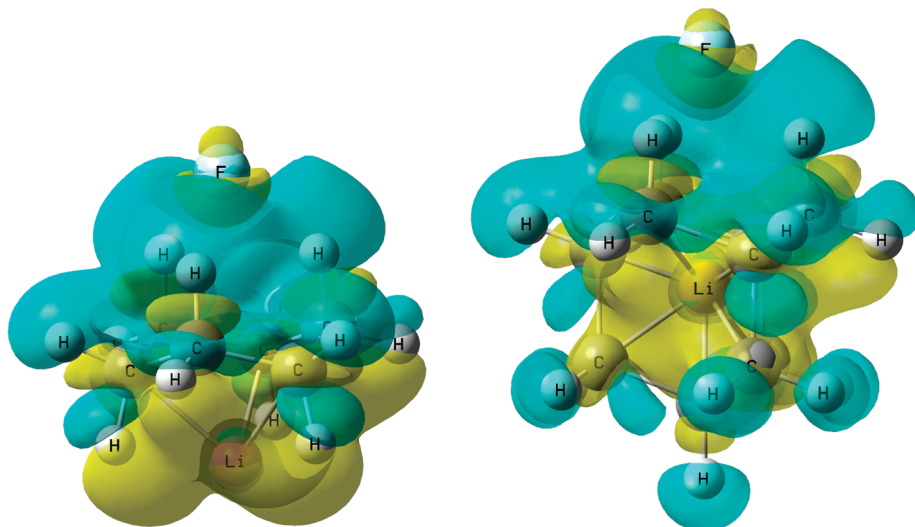


Figure 6. Electron density shift of the $\text{F}^-:\text{C}_6\text{H}_{12}:\text{Li}^+$ and $\text{F}^-:\text{C}_{10}\text{H}_{16}:\text{Li}^+$ complexes at $\pm 0.001 \text{ au}$ isosurfaces. Blue and yellow represent lost and gain of electron density respectively.

of the Laplacian. The ρ_{BCP} values obtained in these complexes are larger than those in the hydrocarbon: M^+ ones when X and M belong to the same row of the periodic table.

The charges of the anions indicate a small charge transfer in the complexes with cyclohexane and in those in the outer face of adamantane but, as in the case of the complexes with cations, the charge transfer is larger in the complexes inside the adamantane. The extent of the electron density overlap using the 0.001 au isosurface of the isolated monomers shows, as in the case of the complexes with cations, an inverse relationship with the size of the anion. Thus, the overlap follows the $\text{F}^- > \text{Cl}^- > \text{Br}^-$ pattern. The overlap is larger in the case of adamantane complexes than in

the cyclohexane ones in agreement with the interatomic distances and interaction energies.

X⁻:Hydrocarbon:M⁺ Complexes. The possibility to have the Li^+ cation in one side of the hydrocarbon and the anion in the opposite one has been considered. For the complexes with adamantane only the disposition of the cation inside and the anion outside has been taken into account.

Very large interaction energies are obtained for these complexes (Table 7), especially in those with cyclohexane. Most of the interaction energy obtained corresponds to the cation:anion interaction through the space, which ranges from -333 to -283 kJ mol^{-1} in the cyclohexane complexes and from -422 to -352

kJ mol^{-1} in those of adamantane. A cooperative energy effect can be estimated as indicated in eq 1.

$$\begin{aligned} E_{\text{coop}} &= E_i(\text{X}^- : \text{hydrocarbon} : \text{Li}^+) \\ &- E_i(\text{X}^- : \text{hydrocarbon}) \\ &- E_i(\text{hydrocarbon} : \text{Li}^+) - E_i(\text{X}^- : \text{Li}^+) \end{aligned} \quad (1)$$

where the first three terms have been calculated using the energy of the complexes in their minima configuration and the isolated monomers including the BSSE correction. The last term ($\text{X}^-:\text{Li}^+$) corresponds to the interaction energy of the two ions in the configuration obtained in the $\text{X}^-:\text{hydrocarbon}:\text{Li}^+$ complex.

The values obtained for E_{coop} indicate that the interaction in the trimer is more favorable than the three pairwise interactions in the case of the cyclohexane complexes, but the opposite happens in the case of the adamantane ones. The latter results could be associated to a less effective interaction of the ions in the adamantane trimer and, thus, turning the overall cooperativity positive.

Shorter distances between the ions and the hydrocarbons are obtained in the triads than in the corresponding dyads previously

Table 9. Electron Density Properties of the BCP and Molecular Charges Calculated at the MP2/6-311++G(3df,2p) Level

system	H...X		Li...C		molecular charges		
	ρ	$\nabla^2\rho$	ρ	$\nabla^2\rho$	X^-	$\text{C}_6\text{H}_{12}/\text{C}_{10}\text{H}_{16}$	Li^+
$\text{F}^-:\text{C}_6\text{H}_{12}:\text{Li}^+$	0.0295	0.0103	0.0233	0.1547	-0.899	0.016	0.914
$\text{Cl}^-:\text{C}_6\text{H}_{12}:\text{Li}^+$	0.0183	0.0545	0.0222	0.1464	-0.869	0.048	0.918
$\text{Br}^-:\text{C}_6\text{H}_{12}:\text{Li}^+$	0.0164	0.0434	0.0220	0.1444	-0.866	0.052	0.919
$\text{F}^-:\text{C}_{10}\text{H}_{16}:\text{Li}^+$	0.0298	0.1057	0.0671	0.4803	-0.908	-0.100	0.808
$\text{Cl}^-:\text{C}_{10}\text{H}_{16}:\text{Li}^+$	0.0192	0.0576	0.0642	0.4589	-0.867	-0.053	0.814
$\text{Br}^-:\text{C}_{10}\text{H}_{16}:\text{Li}^+$	0.0170	0.0452	0.0669	0.4792	-0.865	-0.051	0.814

discussed. The largest shortening is obtained in the complexes with the bromide anions with values up to 0.36 Å. In the case of the adamantane complexes, the lithium cation is no longer in the center of the hydrocarbon approaching the face where the anion is located.

The DFT-SAPT partition of the interaction of both ions with the hydrocarbons has been gathered in Table 8. The results show that the exchange term, $E_{\text{ex}}^{(1)}$, is the most important one in absolute value, especially in the complexes with adamantane. Regarding the attractive term, the induction, $E_i^{(2)}$, is slightly more important than the electrostatic one, $E_{\text{el}}^{(1)}$, in the complexes with cyclohexane while in the adamantane ones, the former is about twice the value of the latter. Thus, the values obtained for these complexes include a sum of the characteristics of both cations and anions complexes shown previously.

The topological analysis of the electron density shows the presence of simultaneous interactions between the anions and the cations with the hydrocarbons (Figure 5). However, while in the cyclohexane: Li^+ complexes the bond path connected the cation with the hydrogen atoms, here the bond is formed between the Li^+ and the closest three carbon atoms of cyclohexane. The results obtained in this case present larger values of the electron density at the BCP than those obtained in the corresponding $\text{Li}^+:\text{hydrocarbon}$ and $\text{X}^-:\text{hydrocarbon}$ complexes.

The charges calculated for each molecule within the triads show that the electron transfer in these cases is much larger than those in the corresponding dyads and a larger neutralization of the ions is observed. Even though the total charge of the hydrocarbons is small compared to that of the ions, it is clear from the electron density shift maps (Figure 6) that they play a very important role in the electron transfer between the anions and lithium cation. Thus, all the hydrogen atoms not involved directly in the interaction suffer an important loss of electron density while the carbon atoms, especially in adamantane, gain it. This effect could be the responsible of a less effective anion/cation

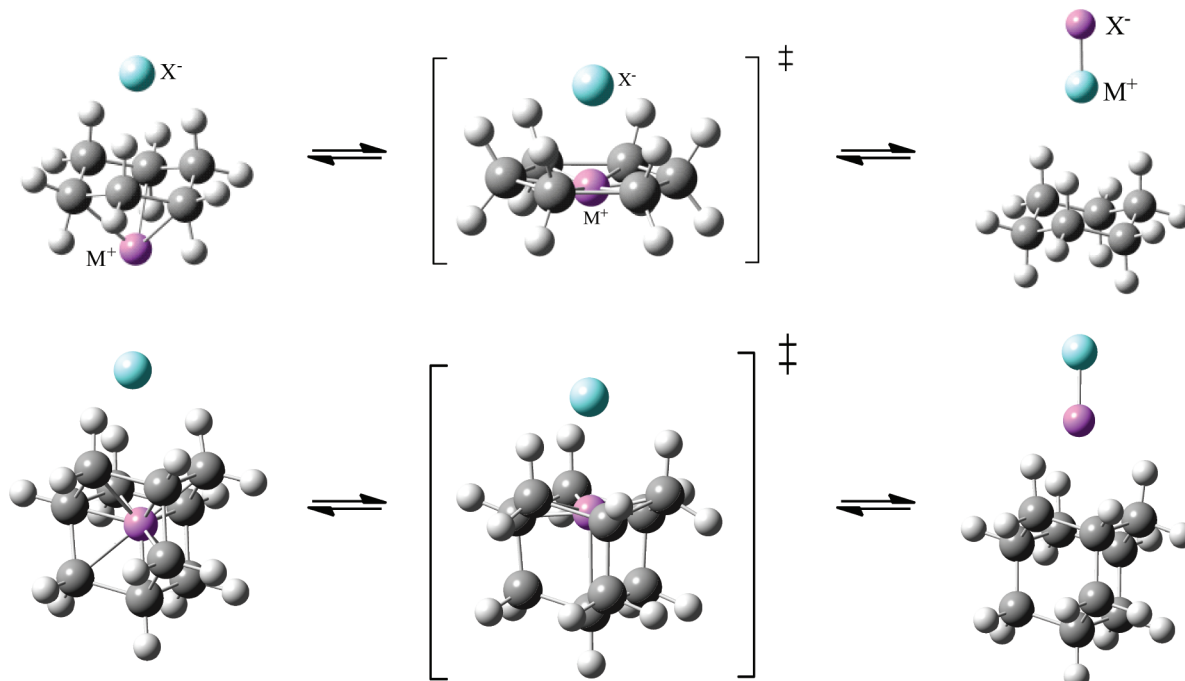


Figure 7. Scheme of the stationary points studied in the lithium cation hydrocarbon crossing in the presence of anions.

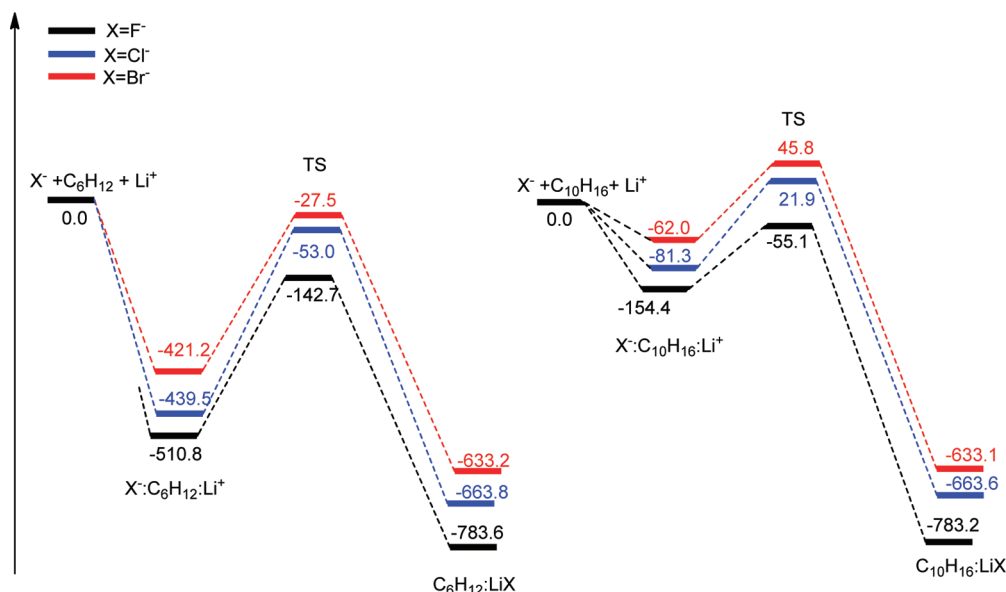


Figure 8. Scheme of the relatives energies in kJ mol^{-1} at the MP2/6-311++G(3df,2p) level using as reference values of the entrance channel.

interaction in the adamantane trimers that results in an anticooperativity effect.

In addition, the possibility that the lithium cations cross the hydrocarbon and form the corresponding LiX salt has been explored (Figure 7). The overall energetic shape of this transformation is shown in Figure 8 with respect to the entrance channel energies. In the case of the cyclohexane complexes, all the stationary points considered have an energy below the entrance channel and thus, the process can evolve spontaneously from the initial components. Regarding the adamantane complexes, only in the case of the fluoride anion ones, are all the stationary points below the entrance channel, while the TS of chloride and bromide show small positive values. The relative energies of each stationary point show a similar tendency, the most negative values being those of the fluoride anion, followed by chloride, and those of bromide being the less negative (or more positive). The TS barriers with respect to the complexes formed are between -27 and -143 kJ/mol in the cyclohexane cases and $+46$ and -55 kJ mol^{-1} in the adamantane ones. The smallest barrier in the adamantane complexes can be explained based on the larger strain observed for these structures which destabilizes the complex with the lithium cation inside.

The formation of the LiX salt is a very favorable process as indicated by the large negative energy values of the final complexes formed.

Regarding the geometry of the systems in the TS, it is worth mentioning that the C–C distances of the hydrocarbons increase, for example, in the cyclohexane with $X^- = F^-$, the C–C distances in the TS vary from 1.548 to 1.700 Å.

CONCLUSIONS

A theoretical study of the interactions of anions and cations with hydrocarbons (cyclohexane as a model of graphane and adamantane as a model of diamondoids) has been carried out at the MP2 computational level. The disposition and interaction energies of the anion:hydrocarbon complexes are similar to those of the cation:hydrocarbon in the case of cyclohexane and in the outer face of adamantane complexes with anions and cations of

the same row of the periodic system. Inside the adamantane, only the lithium cation shows acceptable energies to be experimentally observed.

The barrier for the lithium cation to cross from one face of the hydrocarbons to the other one has been calculated showing very large values.

The lithium:hydrocarbon:anions complexes have large interaction energies mostly due to the interactions of the ions across the space. The calculated barriers of the lithium crossing the hydrocarbons are below the energy of the isolated molecules in the case of the cyclohexane complexes and in the $\text{Li}^+:\text{C}_{10}\text{H}_{16};\text{F}^-$ one and slightly above this level in the $\text{Li}^+:\text{C}_{10}\text{H}_{16};\text{Cl}^-$ and $\text{Li}^+:\text{C}_{10}\text{H}_{16};\text{Br}^-$ cases. The formation of the lithium salt is a very favorable process.

The DFT-SAPT analysis indicates that the dominant term is the induction one in the complexes with the cations while the repulsion-exchange is the most important component in the complexes with the anions and in those with the cations and anions in different faces of the hydrocarbons.

AUTHOR INFORMATION

Corresponding Author

*E-mail: ibon@iqm.csic.es. Web: <http://www.iqm.csic.es/are>.

ACKNOWLEDGMENT

We thank the Ministerio de Ciencia e Innovación (Project No. CTQ2009-13129-C02-02), the Spanish MEC (CTQ2007-62113), and the Comunidad Autónoma de Madrid (Project MADRISOLAR2, ref S2009/PPQ-1533) for continuing support. Thanks are given to the CTI (CSIC) for an allocation of computer time.

REFERENCES

- (1) Mikhailov, S. *Physics and applications of graphene—experiments*; InTech: Rijeka (Croatia), 2011.
- (2) Heller, A. *J&TR* 2008, March/April, 14-16.

- (3) Sofo, J. O.; Chaudhari, A. S.; Barber, G. D. *Phys. Rev. B* **2007**, *75*, 153401.
- (4) Samarakoon, D. K.; Wang, X.-Q. *ACS Nano* **2009**, *3*, 4017–4022.
- (5) Wen, X.-D.; Hoffmann, R.; Ashcroft, N. W. *J. Am. Chem. Soc.* **2011**, *133*, 9023–9035.
- (6) Farah, M.; Kavoos, M. *J. Phys.: Condens. Matter* **2009**, *21*, 215303.
- (7) Duan, Z.; Wang, Z.; Gao, S. *Dalton Trans.* **2011**, *40*, 4465–4473.
- (8) Drut, J., E.; Lähde, T. A. *Phys. Rev. Lett.* **2009**, *102*, 026802.
- (9) Sugawara, K.; Kanetani, K.; Sato, T.; Takahashi, T. *AIP Adv.* **2011**, *1*, 022103–022105.
- (10) Ma, J. C.; Dougherty, D. A. *Chem. Rev.* **1997**, *97*, 1303–1324.
- (11) Gallivan, J. P.; Dougherty, D. A. *Proc. Natl. Acad. Sci. U.S.A.* **1999**, *96*, 9459–9464.
- (12) Meyer, E. A.; Castellano, R. K.; Diederich, F. *Angew. Chem., Int. Ed.* **2003**, *42*, 1210–1250.
- (13) Mascal, M.; Armstrong, A.; Bartberger, M. D. *J. Am. Chem. Soc.* **2002**, *124*, 6274–6276.
- (14) Alkorta, I.; Rozas, I.; Elguero, J. *J. Am. Chem. Soc.* **2002**, *124*, 8593–8598.
- (15) Quiñonero, D.; Garau, C.; Rotger, C.; Frontera, A.; Ballester, P.; Costa, A.; Deyà, P. M. *Angew. Chem., Int. Ed.* **2002**, *41*, 3389–3392.
- (16) Frontera, A.; Quiñonero, D.; Deyà, P. M. *WIREs Comput. Mol. Sci.* **2011**, *1*, 440–459.
- (17) Garau, C.; Quiñonero, D.; Frontera, A.; Ballester, P.; Costa, A.; Deyà, P. M. *New J. Chem.* **2003**, *27*, 211–214.
- (18) Alkorta, I.; Elguero, J. *J. Phys. Chem. A* **2003**, *107*, 9428–9433.
- (19) Alkorta, I.; Quiñonero, D.; Garau, C.; Frontera, A.; Elguero, J.; Deyà, P. M. *J. Phys. Chem. A* **2007**, *111*, 3137–3142.
- (20) Quiñonero, D.; Frontera, A.; Deyà, P. M.; Alkorta, I.; Elguero, J. *Chem. Phys. Lett.* **2008**, *460*, 406–410.
- (21) Alkorta, I.; Blanco, F.; Deyà, P. M.; Elguero, J.; Estarellas, C.; Frontera, A.; Quinonero, D. *Theor. Chem. Acc.* **2010**, *126*, 1–14.
- (22) Kim, D.; Lee, E. C.; Kim, K. S.; Tarakeshwar, P. *J. Phys. Chem. A* **2007**, *111*, 7980–7986.
- (23) Albertí, M.; Aguilar, A.; Pirani, F. *J. Phys. Chem. A* **2009**, *113*, 14741–14748.
- (24) Zhu, L.; Wang, S.; Li, Y.; Zhang, Z.; Hou, H.; Qin, Q. *Appl. Phys. Lett.* **1994**, *65*, 702–704.
- (25) Varshni, Y. P. *Phys. B (Amsterdam, Neth.)* **2001**, *307*, 197–202.
- (26) Stevenson, C. D.; Noyes, J. R.; Reiter, R. C. *J. Am. Chem. Soc.* **2000**, *122*, 12905–12906.
- (27) Liu, Z. *Int. J. Hydrogen Energy* **2007**, *32*, 3987–3989.
- (28) Aoyagi, S.; Nishibori, E.; Sawa, H.; Sugimoto, K.; Takata, M.; Miyata, Y.; Kitaura, R.; Shinohara, H.; Okada, H.; Sakai, T.; Ono, Y.; Kawachi, K.; Yokoo, K.; Ono, S.; Omote, K.; Kasama, Y.; Ishikawa, S.; Komuro, T.; Tobita, H. *Nat. Chem.* **2010**, *2*, 678–683.
- (29) Moran, D.; Woodcock, H. L.; Chen, Z.; Schaefer, H. F.; Schleyer, P. v. R. *J. Am. Chem. Soc.* **2003**, *125*, 11442–11451.
- (30) Bader, R. F. W.; Fang, D.-C. *J. Chem. Theory Comput.* **2005**, *1*, 403–414.
- (31) Wang, S.-G.; Qiu, Y.-X.; Schwarz, W. H. E. *Chem.—Eur. J.* **2010**, *16*, 9107–9116.
- (32) Frisch, M. J.; Pople, J. A.; Binkley, J. S. *J. Chem. Phys.* **1984**, *80*, 3265–3269.
- (33) Møller, C.; Plesset, M. S. *Phys. Rev.* **1934**, *46*, 618–622.
- (34) Boys, S. F.; Bernardi, F. *Mol. Phys.* **1970**, *19*, 553–566.
- (35) Chalański, G.; Szczęśniak, M. M. *Chem. Rev.* **2000**, *100*, 4227–4252.
- (36) Werner, H.-J.; Knowles, P. J.; Manby, F. R.; Schütz, M.; Celani, P.; Knizia, G.; Korona, T.; Lindh, R.; Mitrushenkov, A.; Rauhut, G.; Adler, T. B.; Amos, R. D.; Bernhardsson, A.; Berning, A.; Cooper, D. L.; Deegan, M. J. O.; Dobbyn, A. J.; Eckert, F.; Goll, E.; Hampel, C.; Hesselmann, A.; Hetzer, G.; Hrenar, T.; Jansen, G.; Köppl, C.; Liu, Y.; Lloyd, A. W.; Mata, R. A.; May, A. J.; McNicholas, S. J.; Meyer, W.; Mura, M. E.; Nicklass, A.; Palmieri, P.; Pfüger, K.; Pitzer, R.; Reiher, M.; Shiozaki, T.; Stoll, H.; Stone, A. J.; Tarroni, R.; Thorsteinsson, T.; Wang, M.; Wolf, A. *MOLPRO*; Cardiff, U.K., 2010.
- (37) Bader, R. F. W. *Atoms in Molecules: A Quantum Theory*; Clarendon Press: Oxford, 1990.
- (38) Popelier, P. L. A. *Atoms In Molecules. An introduction*; Prentice Hall: Harlow, England, 2000.
- (39) Biegler-König, F. W.; Bader, R. F. W.; Tang, T. H. *J. Comput. Chem.* **1982**, *3*, 317–328.
- (40) Popelier, P. L. A. *Chem. Phys. Lett.* **1994**, *228*, 160–164.
- (41) Rafat, M.; Popelier, P. L. A. *J. Comput. Chem.* **2007**, *28*, 2602–2617.
- (42) Reed, A. E.; Curtiss, L. A.; Weinhold, F. *Chem. Rev.* **1988**, *88*, 899–926.
- (43) Glendening, E. D.; Reed, A. E.; Carpenter, J. E.; Weinhold, F.
- (44) Kim, D.; Hu, S.; Tarakeshwar, P.; Kim, K. S.; Lisy, J. M. *J. Phys. Chem. A* **2003**, *107*, 1228–1238.
- (45) Soteras, I.; Orozco, M.; Luque, F. *J. Phys. Chem. Chem. Phys.* **2008**, *10*, 2616–2624.
- (46) Carrazana-García, J. A.; Rodríguez-Otero, J.; Cabaleiro-Lago, E. M. *J. Phys. Chem. B* **2011**, *115*, 2774–2782.
- (47) Kim, D.; Tarakeshwar, P.; Kim, K. S. *J. Phys. Chem. A* **2004**, *108*, 1250–1258.
- (48) Koch, U.; Popelier, P. L. A. *J. Phys. Chem.* **1995**, *99*, 9747–9754.